Adsorption Effect Modification of Lithium–Sulfur Batteries

Subjects: Chemistry, Applied

Contributor: Bo-Wen Zhang , Bo Sun , Pei Fu , Feng Liu , Chen Zhu , Bao-Ming Xu , Yong Pan , Chi Chen

Lithium–sulfur batteries (LSBs) have high theoretical specific capacity (1675 mAh g^{-1}) and high energy density (2600 Wh kg^{-1}), and the cathode sulfur is low cost, abundant, and environmentally friendly. The “shuttle effect” refers to the phenomenon that Li_2S_x ($4 \le x \le 8$) produced by the positive electrode diffuses to the negative electrode during the charging and discharging process, and is reduced to solid Li_2S_2/Li_2S on the negative electrode surface and attached to the negative electrode.

lithium–sulfur batteries polysulfide “shuttle effect” separator modification

1. Introduction

Along with the development of mobile electronics and electric vehicles, a trend to develop energy storage devices with high efficiency and high specific energy has emerged [1][2][3]. Rechargeable batteries with long service life and high energy storage efficiency are attracting much attention from researchers. Among them, lithium–sulfur batteries (LSBs) have high theoretical specific capacity (1675 mAh g^{-1}) and high energy density (2600 Wh kg^{-1}) [4][5], and the cathode sulfur is low cost, abundant, and environmentally friendly. Therefore, LSBs have great development prospects [6]. The charge–discharge process of LSBs is a dissolution–deposition reaction [7]. During the discharge process, the cathode sulfur (S_8) is electrochemically reduced to soluble long-chain lithium polysulfide Li_2S_x ($4 \le x \le 8$) first, and then converted to insoluble short-chain Li_2S_2/Li_2S. The charging reaction is the opposite of the discharging reaction. The solid Li_2S_2/Li_2S is first converted to short-chain LiPS, which is then further oxidized to soluble long-chain Li_2S_x ($4 \le x \le 8$), and finally to solid S_8. The reaction is as follows [8]:

$$\text{Negative electrode: } 16\ Li \rightleftharpoons 16\ Li^+ + 16\ e^- \quad (1)$$

$$\text{Positive electrode: } S_8 + 16\ Li^+ + 16\ e^- \rightleftharpoons 8\ Li_2S \quad (2)$$

The “shuttle effect” of LSBs is known to be an important factor limiting their practical application [9][10][11][12]. The “shuttle effect” refers to the phenomenon that Li_2S_x ($4 \le x \le 8$) produced by the positive electrode diffuses to the negative electrode during the charging and discharging process, and is reduced to solid Li_2S_2/Li_2S on the negative electrode surface and attached to the negative electrode. It can cause irreversible loss of battery active material, increase battery internal resistance, and decrease the theoretical capacity of LSBs [13][14][15].

2. Adsorption Effect Modification

2.1. Physical/Chemical Adsorption

The modification of the separator of LSBs by means of the physical adsorption effect generally refers to the use of the van der Waals force between LiPSs and the trapping material to capture LiPSs. Separator materials with high porosity and large specific surface area can provide more trapping sites, which are beneficial to inhibit the migration of LiPSs between the electrodes [16]. Therefore, attaching porous carbon materials such as carbon nanofibers, carbon flakes, microporous carbon nanofibers, reduced graphene oxide, etc. as a coating to the separator has been widely used in the separator modification of LSBs. The modification effects of different carbon materials are shown in **Table 1**. Generally speaking, the high sulfur loading of the cathode will increase more LiPSs in the electrolyte and result in a severer shuttle effect of LSBs. From **Table 1**, it can be seen that the improvement of using light mesoporous carbon as the coating to modify the separator is the most significant. At the high sulfur loading (3.5 mg cm^{-2}), the LSBs with this separator have a mass specific capacity of 1021 mAh g^{-1} after 100 cycles at 0.5 C, with a capacity decay rate of only 0.081%. This may be because the large number of mesopores (12 nm) in the mesoporous carbon can tune the huge volume change of S_8 during the lithiation process, thereby suppressing the loss of polysulfides, which in turn controls the shuttle of LiPSs and improves the electrochemical performance of LSBs.

Table 1. The properties of PP separators modified with different carbon materials in LSBs.

Materials	Total Pore Volume/cm^3 g^{-1}	Surface Area/m^2 g^{-1}	Coating Binder Content	Area Density /mg cm^{-2}	Cathode Sulfur Content/wt%	S Loading/mg cm^{-2}	Capacity/(mAh g^{-1}) (Rate)	Cycling Performance/(mAh g^{-1}) (Cycles, Rate)	Capacity Decay/%	Ref.
Super P	-	-	None	0.2	55	1.1–1.3	1289 (0.5 C)	828 (200/0.2 C)	0.19	[17]
MWCNTs	2.76	410.42	None	0.17	55	-	1107 (0.5 C)	881 (150/0.2 C)	0.14	[18]
PG	3.361	1443	20 wt% PVP	0.54	63	1.8–2.0	1165 (0.5 C)	877 (150/0.5 C)	-	[19]
PC/MWCNT	0.17	83.4	10 wt% PVDF	0.51	70	1.6–1.7	911 (0.5 C)	659 (200/0.5 C)	0.138	[20]
GCFF	-	-	None	-	60	0.7	1280.14 (0.2 C)	1004.62 (100/0.2 C)	-	[21]
CFs	-	-	None	0.16	60	1	1280.14 (0.2 C)	683 (500/0.5 C)	0.071	[22]
rGO/CB	2.334	861.12	None	-	-	-	1014.5 (0.2 C)	850.9 (100/0.2 C)	0.17	[23]
CNT/AC	0.19	1312	20 wt% PVDF	-	70	-	1495.6 (0.2 C)	742 (200/0.2 C)	0.25	[24]

Materials	Total Pore Volume/cm^3 g^{-1}	Surface Area/m^2 g^{-1}	Coating Binder Content	Area Density /mg cm^{-2}	Cathode Sulfur Content/wt%	S Loading/mg cm^{-2}	Capacity/(mAh g^{-1}) (Rate)	Cycling Performance/(mAh g^{-1}) (Cycles, Rate)	Capacity Decay/%	Ref.
HCNF/rGO	-	-	None	1.2 [27]	60	1.4	1318.4 (0.2 C)	779.1(100/1 C)	0.13	[25]
mesoC	2.9	843	5 wt% super P and 10 wt% PVDF-HFP	0.5	70	3.5	1378 (0.2 C)	1021 (100/0.5 C)	0.081	[26]

capacity
arator by
ator with
nibited a

Chu et al. [28] modified the PP separator of LSBs with a mixture of ethylene oxide (PEO) and lithium bis(trifluoromethanesulfonyl)imide (LiTFSI) as a coating. The experimental results show that the lithium-ion diffusion coefficient (9.6×10^{-9}~3.0×10^{-8} cm^2 s^{-1}) of PEO/LiTFSI coating is significantly higher than that of pure PP separator (7.6×10^{-9}~2.2×10^{-8} cm^2 s^{-1}). The LSBs with PEO/LiTFSI separator achieve an initial discharge capacity of 1212 mAh g^{-1} at 0.1 C and can still maintain a high reversible capacity of 534 mAh g^{-1} and a stable coulombic capacity after 200 cycles. This may be due to the fact that PEO can inhibit the diffusion of LiPSs as a gel polymer electrolyte, and the addition of LiTFSI salt enhances the ability of the lithium ion transfer of the PEO coating. The electrochemical efficiency and the synergistic effect of the PEO/LiTFSI coating are shown in **Figure 1**.

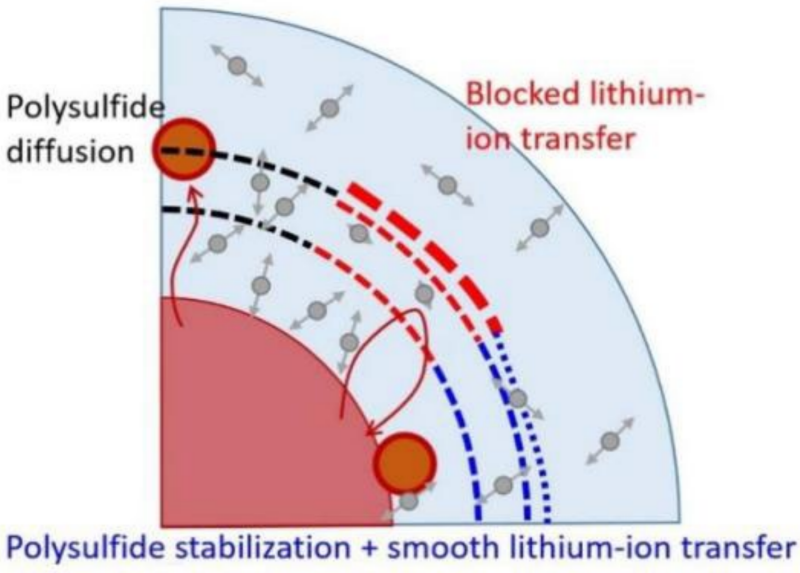

Figure 1. Schematic diagram of PEO/LiTFSI coating hindering LiPSs [28].

Although the modification of polyolefin separators with carbon materials can inhibit the shuttle of LiPSs between the two electrodes of LSBs to a certain extent, the interaction force between non-polar carbon materials and polar LiPSs is weak. Therefore, inhibiting the diffusion of LiPSs in the LSBs only by physical adsorption is not satisfied [29]. Compared with physical adsorption, chemical adsorption, which relies on the formation of chemical bonding forces between LiPSs and the surface atoms of adsorbent materials, can make a higher selectivity and achieve a better immobilizing effect of LiPSs [30]. For example, doping electronegative heteroatoms (such as N, O, and S, etc.) in carbon coatings can help trap LiPSs by the formation of Li–X bonds (dipole–dipole interactions) between heteroatoms and LiPSs [31][32]. Hou et al. [33] analyzed the ability of various atomically doped graphene

nanoribbons (GNRs) to adsorb sulfur and Li_2S_x by density functional theory (DFT). It was found that the adsorption effect of N and O (binding energy −2.53~−2.56 eV)-doped GNRs on Li_2S_4 is much greater than that of B, F, S, P, and Cl (binding energy −1.93 eV), which is due to the existence of dipole–dipole electrostatic interactions (~1.95 eV). The relationship between element electronegativity and binding energy is shown in **Figure 2**.

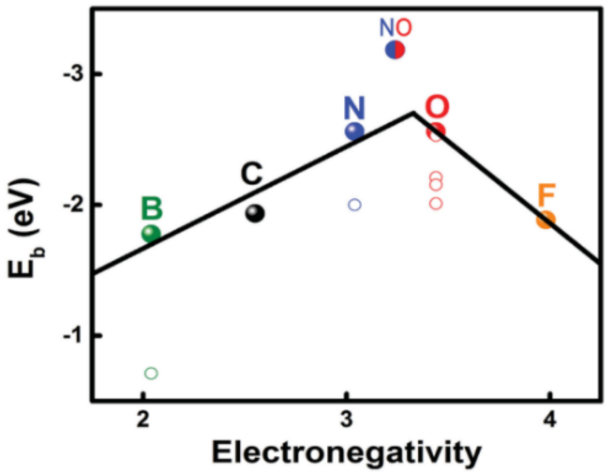

Figure 2. The relationship between the binding energy (E_b) of the doping element−Li_2S_4 and the electronegativity of the element [33].

Zeng et al. [34] designed a honeycomb-like N, P diatomic doped carbon (HNPC) modified separator, in which the HNPC coating can effectively anchor the LiPSs by forming N–Li and P–S bonds. When using the acetylene black-sulfur composite as the cathode with the sulfur content of 79.7%, the LSBs showed excellent long-cycle stability with a capacity decay rate of only 0.06% per cycle after 900 cycles at 1 C. **Figure 3** shows the cycle performance of separators modified by different coatings. It can be seen that the chemical confinement of LiPSs by diatomic doping is higher than that of single-atom doping systems.

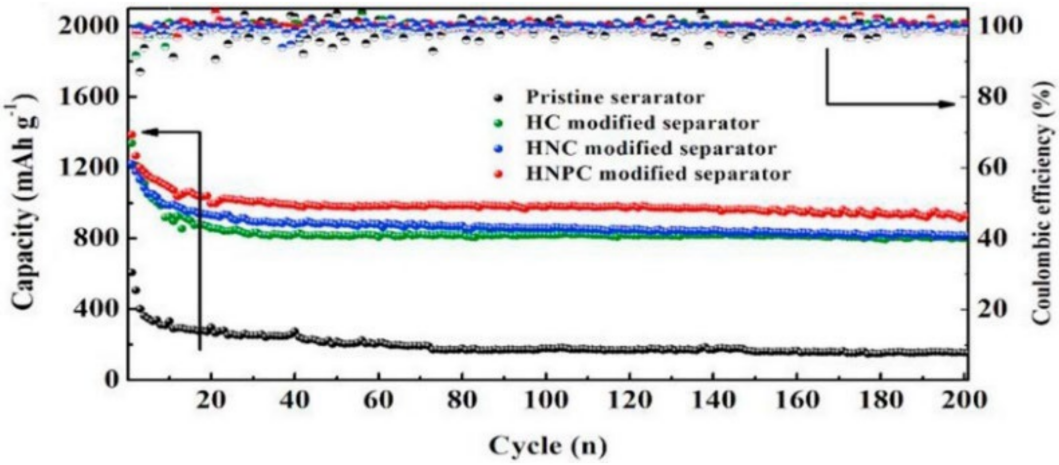

Figure 3. Cycle performance of LSBs using different separators at 0.2 C [34].

Besides polar atoms, the doping of polar functional groups can also realize the chemisorption of the separator to LiPSs. Pei et al. [35] used polydopamine/polyethylene oxide (PDA/PEI) to modify polyolefin separators and achieved desired results. The PDA/PEI-modified separator made the initial discharge capacity of LSBs 1250 mAh g^{-1} at 0.2 C and it remained900 mAh g^{-1} after 100 cycles. This could be attributed to the formation of numerous C=N bonds between the amine groups in PEI and dopamine, which inhibited the accumulation of dopamine oligomers on the separator through hydrogen bonds or π−π bonds, thereby making the separator hydrophilic, and the enriched N and O functional groups of the PDA/PEI coating effectively adsorbed LiPSs in the electrolyte.

In addition, the modification of PP separator with metal materials, metal oxides, and metal sulfides, the exposed metal (M) sites of which can form S–M bonds with LiPSs, are also beneficial to improve its adsorption capacity to LiPSs [36]. Tao et al. [12] calculated by DFT that the binding energy of metal oxides and LiPSs (from −1.54 to −7.12 eV), is higher than that of heteroatoms and LiPSs (from −2.53 to −2.56 eV). Liu et al. [37] designed graphene oxide (GO) coatings doped with TiO_2 nanoparticles, as shown in **Figure 4**a. The Ti–O–C bond formed between TiO_2 and GO and the wrinkled sheet structure of GO make the combination of TiO_2 and GO tight, which helps to enhance the electrical conductivity of the separator. Meanwhile, the S–Ti–O and Ti–S bonds formed between TiO_2 and S enhanced the ability of the separator to adsorb LiPSs. The LSBs coated with TiO_2/GO separator can retain a reversible capacity of 843.4 mAh g^{-1} after 100 cycles at 0.2 C (**Figure 4**b).

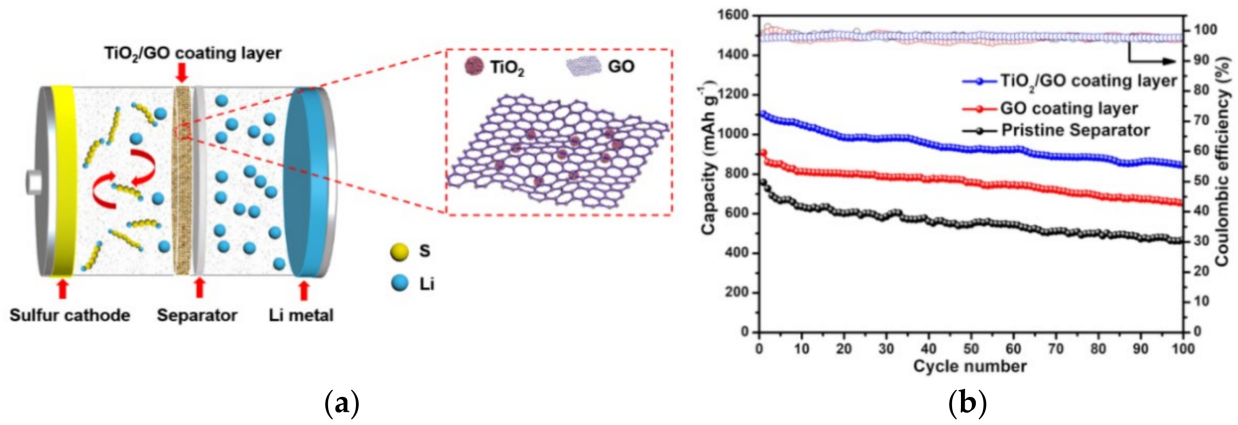

Figure 4. (**a**) Schematic diagram of LBSs with TiO_2/GO coated functional separator. (**b**) Cyclic performance and coulombic efficiency of the LSBs batteries with different coated separators at a rate of 0.2 C [37].

2.2. Catalytic Adsorption

Physical/chemical adsorption can suppress the “shuttle effect” of LiPSs, but under the conditions of high sulfur loading (>5 mg cm^{-2}) or long cycling, the increase of LiPSs dissolved in the electrolyte will lead to slow reaction kinetics. Moreover, the limited adsorption sites on the separator are not enough to adsorb LiPSs in the electrolyte fully, thus resulting in a low specific capacity and short cycle life of the battery. Therefore, the ability of the separator to suppress the “shuttle effect” may be reduced or even lost [38][39]. The introduction of catalytic substances on the surface of the separator can not only reduce the energy barrier of the conversion of LiPSs and insoluble Li_2S_2/Li_2S, accelerating the electrochemical reaction of LSBs, but also transfer the adsorbed LiPSs to the

redox reaction in time. Thus, the content of the active substances of the battery is kept to the greatest extent, and the cycle performance of LSB is significantly improved [14].

Inherent defects in the metal oxide structure can provide more active sites for trapping and transforming LiPSs [40]. Lv et al. [41] loaded bimetallic $NiCo_2O_4$ nanoparticles onto reduced graphene oxide as a catalytic coating for the separator. During the electrode reaction process, the oxidized metal ions (Ni^{3+} and Co^{3+}) combine with LiPSs to form Ni–S and Co–S bonds, which anchor the LiPSs to the $NiCo_2O_4$@rGO surface to suppress the "shuttle effect" of LBSs. Furthermore, DFT calculations show that the $NiCo_2O_4$ (100) crystal surface has a low Li-ion diffusion barrier (0.15 eV compared to 0.293 eV for carbon materials), which helps to improve the migration rate of lithium ions and promote lithium-ion–electron coupling, thereby accelerating the conversion of LiPSs to Li_2S_2/Li_2S. Using a core-shell structure material (encapsulated sulfur in carbon) with a sulfur content of 70 wt% as the cathode and under the condition of a high sulfur loading of 6 mg cm^{-2}, the LBSs showed the capacity loss rate only 0.02% after 400 cycles at a current density of 1 mA cm^{-2}, and at the same time, there was an excellent areal capacity of 7.1 mAh cm^{-2}.

Adding other metals to monometallic compounds can also improve the reaction kinetics of LiPS transformation on the surface of metal compounds [42]. Zhang et al. [43] introduced Mo atoms into Ni_3N and used a composite of multi-walled carbon nanotubes and $Ni_{0.2}Mo_{0.8}N$ to modify the separator. During the electrochemical reaction process, the Mo atoms in the $Ni_{0.2}Mo_{0.8}N$ are etched and leached out by LiPSs, leaving a large number of vacancies around Ni (**Figure 5**a). The vacancies formed can accelerate the charge transfer and the LiPS conversion. The potential of the Ni_3N and Mo_2N surfaces in the coating is higher than lithium negative electrode, thus creating an electric field between the separator and the lithium anode (**Figure 5**b), which promotes the directional movement of sulfur and lithium ions and inhibits the shuttling of LiPSs to some extent. The LSBs with this separator can achieve an initial battery capacity of 1097.2 mAh g^{-1} at a high rate of 5 C.

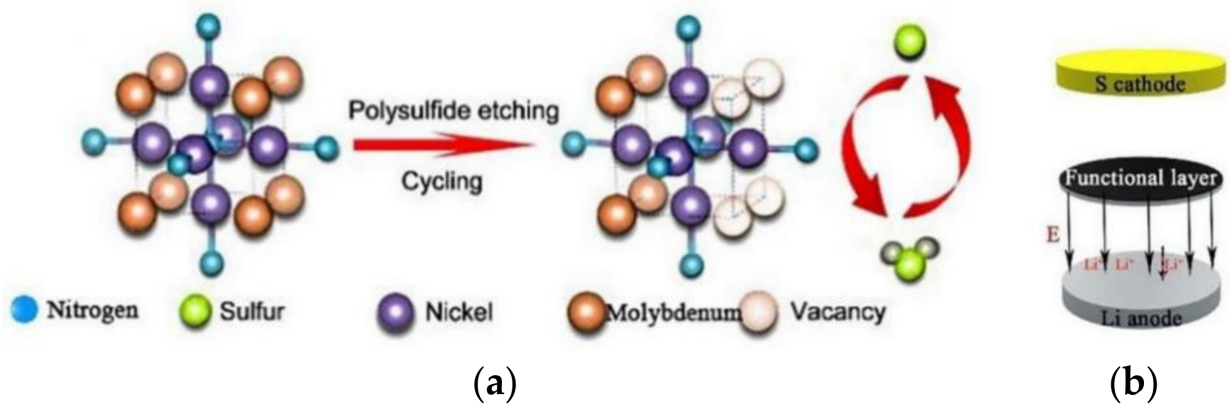

Figure 5. (**a**) Mechanism of in-situ etching of LiPSs by bimetallic nitride. (**b**) Direction of the electric field inside the LSBs [43].

Due to the abundant pore structures and catalytic sites, metal–organic frameworks (MOFs) composed of organic ligands and transition metal ions have been widely used for catalytic modification of the separators of LBSs. The

pore structure in MOFs can promote the adequate contact between the separator and the electrolyte and limits the diffusion of LiPSs, while the metal central ions can chemisorb and catalyze LiPSs [33]. Hong et al. [44] doped cerium-based metal-organic frameworks (Ce-MOFs) into CNTs to form Ce-MOFs/CNT separator coatings. The large specific surface area of Ce-MOFs and the ligated unsaturated Ce (IV) cluster nodes can rapidly adsorb LiPSs and accelerate the conversion between LiPSs and Li_2S_2/Li_2S, which is shown in **Figure 6**a. As seen, under the high sulfur loading of 6 mg cm^{-2}, the initial specific capacity of LSBs was 1021.8 mAh g^{-1} at 1 C, which slowly decreased to 838.8 mAh g^{-1} after 800 cycles with a decay rate of only 0.022% per cycle, as shown in **Figure 6**b. The coulombic efficiency of the LBSs was close to 100%, which suggesting its excellent cycle performance.

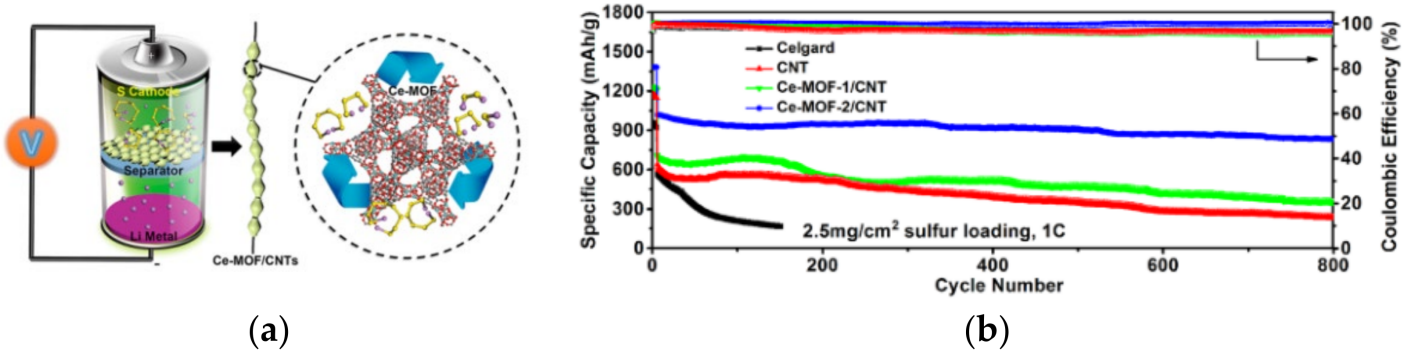

Figure 6. (**a**) Schematic representation of the catalytic conversion of LiPSs on the surface of Ce-MOFs/CNT separators. (**b**) Cyclic performance of cells with different separator at 1 C for 800 cycles (2.5 mg/cm^2 sulfur loading) [44].

In addition to transition metal elements, rare-earth elements have also been used in the catalytic modification of the separators of LBSs. Peng et al. [45] prepared a novel pp separator coated with Eu_2O_3/Ketjen black (Eu_2O_3/KB). The exposed (222) plane of Eu_2O_3 exhibits strong polarity-polarity interaction with LiPSs, which is beneficial to confine the transfer of LiPSs. The adsorption energy of Eu_2O_3 with LiPSs is shown in **Figure 7**. Apart from that, oxygen vacancies in Eu_2O_3 can provide more catalytic sites for regulating Li_2S precipitation. Therefore, with high crystal face index, Eu_2O_3 can lower the energy barrier for Li_2S nucleation on it and promote the conversion of LiPSs to Li_2S. The LBSs with Eu_2O_3/KB modified separator exhibited excellent cycling stability and rate capability. Its capacity decay rate achieved only 0.05% per cycle during 500 cycles at 1 C.

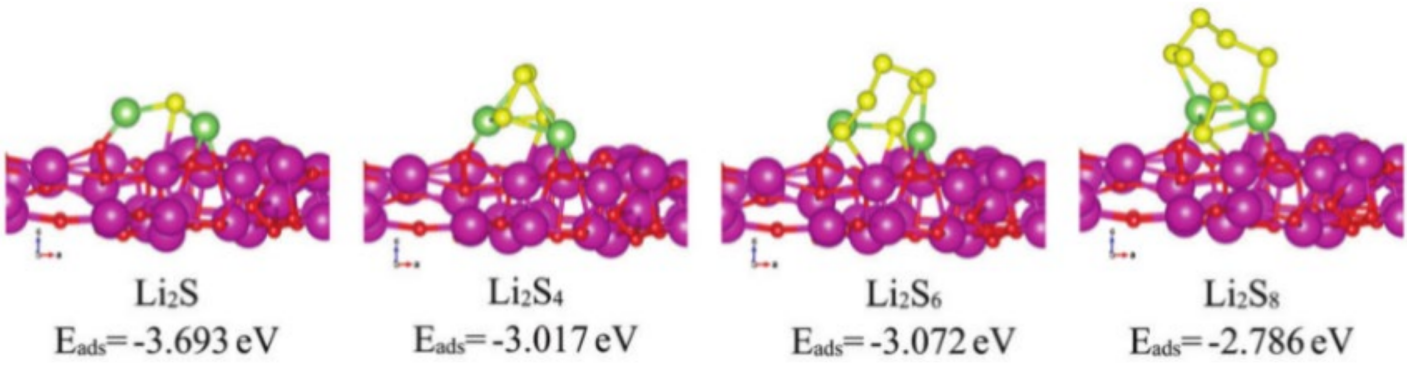

Figure 7. Adsorption energies of different LiPSs on the Eu_2O_3 (222) plane [45].

Some non-metallic materials with catalytic activity have also been used in the separator of LBSs to promote the conversion of LiPSs. For example, Wang et al. [46] used red phosphorus (RP) as a coating to enhance the sulfur reaction kinetics of LSBs.

References

1. Islam, M.S.; Nazar, L.F. Advanced materials for lithium batteries. J. Mater. Chem. 2011, 21, 9810.
2. Ma, Y.; Xie, X.B.; Yang, W.Y.; Yu, Z.P.; Sun, X.Q.; Zhang, Y.P.; Yang, X.Y.; Kimura, H.; Hou, C.X.; Guo, Z.H.; et al. Recent advances in transition metal oxides with different dimensions as electrodes for high-performance supercapacitors. Adv. Compos. Hybrid Mater. 2021, 4, 906–924.
3. Zhai, I.Y.; Yang, W.; Xie, X.; Yu, Z.P.; Sun, X.Q.; Zhang, Y.P.; Yang, X.Y.; Kimura, H.; Hou, C.X.; Guo, Z.H.; et al. Co3O4 nanoparticle-dotted hierarchical-assembled carbon nanosheet framework catalysts with the formation/decomposition mechanisms of Li2O2 for smart lithium–oxygen batteries. Inorg. Chem. Front. 2022, 9, 1115–1124.
4. Ould, E.T.; Kamzabek, D.; Chakraborty, D.; Doherty, M.F. Lithium–sulfur batteries: State of the art and future directions. ACS Appl. Energy Mater. 2018, 1, 1783–1814.
5. Chen, H.; Wang, C.; Dong, W.; Lu, W.; Du, Z.L.; Chen, L.W. Monodispersed sulfur nanoparticles for lithium–sulfur batteries with theoretical performance. Nano Lett. 2015, 15, 798–802.
6. Zhao, M.; Li, B.Q.; Zhang, X.Q.; Huang, J.Q.; Zhang, Q. A perspective toward practical lithium–sulfur batteries. ACS Cent. Sci. 2020, 6, 1095–1104.
7. Li, G.; Wang, S.; Zhang, Y.; Li, M.; Chen, Z.W.; Lu, J. Revisiting the role of polysulfides in lithium–sulfur batteries. Adv. Mater. 2018, 30, 1705590.
8. Abbas, S.A.; Ding, J.; Wu, S.H.; Fang, J.; Boopathi, K.M.; Mohapatra, A.; Lee, L.W.; Wang, P.C.; Chang, C.C.; Chu, C.W. Modified separator performing dual physical/chemical roles to inhibit polysulfide shuttle resulting in ultrastable Li–S batteries. ACS Nano 2017, 11, 12436–12445.
9. He, Y.; Qiao, Y.; Chang, Z.; Cao, X.; Jia, M.; He, P.; Zhou, H. Developing A “Polysulfide-Phobic” Strategy to Restrain Shuttle Effect in Lithium-Sulfur Batteries. Angew. Chem. 2019, 58, 11774–11778.
10. Yan, J.; Liu, X.; Li, B. Capacity Fade Analysis of Sulfur Cathodes in Lithium-Sulfur Batteries. Adv. Sci. 2016, 3, 1600101–1600111.
11. Li, T.; Bai, X.; Gulzar, U.; Bai, Y.J.; Capiglia, C.; Deng, W.; Zhou, X.F.; Liu, Z.P.; Feng, Z.F.; Zaccaria, R.P. A Comprehensive Understanding of Lithium–Sulfur Battery Technology. Adv. Funct.

Mater. 2019, 29, 1901730.

12. Tao, X.; Wang, J.; Liu, C.; Wang, H.; Yao, H.; Zheng, G.Y.; Seh, Z.W.; Cai, Q.X.; Li, W.Y.; Zhou, G.; et al. Balancing surface adsorption and diffusion of lithium-polysulfides on nonconductive oxides for lithium-sulfur battery design. Nat. Commun. 2016, 7, 11203.
13. Manthiram, A.; Fu, Y.; Su, Y.S. Challenges and prospects of lithium–sulfur batteries. Acc. Chem. Res. 2013, 46, 1125–1134.
14. Manthiram, A.; Chung, S.H.; Zu, C. Lithium–sulfur batteries: Progress and prospects. Adv. Mater. 2015, 27, 1980–2006.
15. Dent, M.; Jakubczyk, E.; Zhang, T.; Lekakou, C. Kinetics of sulphur dissolution in lithium–sulphur batteries. J. Phys. Energy 2022, 4, 024001.
16. Liao, H.Y.; Zhang, H.Y.; Hong, H.Q.; Li, Z.H.; Lin, Y.X. Novel flower-like hierarchical carbon sphere with multi-scale pores coated on PP separator for high-performance lithium-sulfur batteries. Electrochim. Acta 2017, 257, 210–216.
17. Chung, S.H.; Manthiram, A. Bifunctional Separator with a Light-Weight Carbon-Coating for Dynamically and Statically Stable Lithium-Sulfur Batteries. Adv. Funct. Mater. 2014, 24, 5299–5306.
18. Chung, S.H.; Manthiram, A. High-Performance Li-S Batteries with an Ultra-lightweight MWCNT-Coated Separator. J. Phys. Chem. Lett. 2014, 5, 1978–1983.
19. Zhai, P.Y.; Peng, H.J.; Cheng, X.B.; Zhu, L.; Huang, J.Q.; Zhu, W.C.; Zhang, Q. Scaled-up fabrication of porous-graphene-modified separators for high-capacity lithium–sulfur batteries. Energy Storage Mater. 2017, 7, 56–63.
20. Tan, L.; Li, X.H.; Wang, Z.X.; Guo, H.J.; Wang, J.X.; An, L. Multifunctional Separator with Porous Carbon/Multi-Walled Carbon Nanotube Coating for Advanced Lithium−Sulfur Batteries. Chemelectrochem 2018, 5, 71–77.
21. Lee, D.K.; Ahn, C.W.; Jeon, H.J. Web-structured graphitic carbon fiber felt as an interlayer for rechargeable lithium—sulfur batteries with highly improved cycling performance. J. Power Sources 2017, 360, 559–568.
22. Zhang, B.; Yu, L.; Zhao, Y. Ultralight carbon flakes modified separator as an effective polysulfide barrier for lithium-sulfur batteries. Electrochim. Acta 2019, 295, 910–917.
23. Zhang, K.M.; Dai, L.Q.; Xie, L.J.; Kong, Q.Q.; Su, F.Y.; Shi, J.; Liu, Y.Z. Graphene/Carbon Black Co-modified Separator as Polysulfides Trapper for Li-S Batteries. Chemistryselect 2019, 4, 6026–6034.
24. Guo, Y.F.; Xiao, J.R.; Hou, Y.X.; Wang, Z.Y.; Jiang, A.H. Carbon nanotube doped active carbon coated separator for enhanced electrochemical performance of lithium–sulfur batteries. J. Mater.

Sci. Mater. Electron. 2017, 28, 17453–17460.

25. Zhang, Z.A.; Wang, G.C.; Lai, Y.Q.; Li, J. A freestanding hollow carbon nanofiber/reduced graphene oxide interlayer for high-performance lithium–sulfur batteries. J. Alloys Compd. 2016, 663, 501–506.
26. Balach, J.; Jaumann, T.; Klose, M.; Oswald, S.; Eckert, J.; Giebeler, L. Functional Mesoporous Carbon-Coated Separator for Long-Life, High-Energy Lithium-Sulfur Batteries. Adv. Funct. Mater. 2015, 25, 5285–5291.
27. Deng, N.; Wang, Y.; Yan, J.; Ju, J.; Li, Z.J.; Fan, L.L.; Zhao, H.J.; Kang, W.M.; Cheng, B.W. A F-doped tree-like nanofiber structural poly-m-phenyleneisophthalamide separator for high-performance lithium-sulfur batteries. Power Sources 2017, 362, 243–249.
28. Chiu, L.L.; Chung, S.H. A Poly(ethylene oxide)/Lithium bis(trifluoromethanesulfonyl)imide-Coated Polypropylene Membrane for a High-Loading Lithium-Sulfur Battery. Polymers 2021, 13, 535.
29. Fan, Y.; Niu, Z.; Zhang, F.; Zhang, R.; Zhao, Y.; Lu, G. Suppressing the Shuttle Effect in Lithium-Sulfur Batteries by a UiO-66-Modified Polypropylene Separator. ACS Omega 2019, 4, 10328–10335.
30. Li, N.; Xie, Y.; Peng, S.T.; Xiong, X.; Han, K. Ultra-lightweight Ti3C2T MXene modified separator for Li–S batteries: Thickness regulation enabled polysulfide inhibition and lithium ion transportation. J. Energy Chem. 2020, 42, 116–125.
31. Zuo, X.; Zhen, M.; Wang, C. graphene nanosheets and CNTs hybrids modified separator as efficient polysulfide barrier for high-performance lithium sulfur batteries. Nano Res. 2019, 12, 829–836.
32. Li, P.Y.; Lv, H.W.; Li, Z.L.; Meng, H.P.; Lin, Z.; Wang, R.H.; Li, X.J. The Electrostatic Attraction and Catalytic Effect Enabled by Ionic-Covalent Organic Nanosheets on MXene for Separator Modification of Lithium-Sulfur Batteries. Adv. Mater. 2021, 33, 2007803.
33. Hou, T.Z.; Chen, X.; Peng, H.J.; Huang, J.Q.; Li, B.Q.; Zhang, Q.; Li, B. Design Principles for Heteroatom-Doped Nanocarbon to Achieve Strong Anchoring of Polysulfides for Lithium-Sulfur Batteries. Small 2016, 12, 3283–3291.
34. Zeng, P.; Huang, L.W.; Zhang, X.L.; Zhang, R.X.; Wu, L.; Chen, Y.G. Long-life and high-areal-capacity lithium-sulfur batteries realized by a honeycomb-like N, P dual-doped carbon modified separator. Chem. Eng. J. 2018, 349, 327–337.
35. Pei, C.B.; Li, J.D.; Lv, Z.Z.; Wang, H.M.; Dong, W.; Yao, Y.Y. Inhibiting polysulfides with PDA/PEI-functionalized separators for stable lithium-sulfur batteries. Int. J. Energy Res. 2021, 46, 10099–10110.

36. Zhang, H.; Lin, C.; Hu, X.H.; Zhu, B.K.; Yu, D.S. Effective Dual Polysulfide Rejection by a Tannic Acid/Fe(III) Complex-Coated Separator in Lithium-Sulfur Batteries. ACS Appl. Mater. Interfaces 2018, 10, 12708–12715.
37. Liu, N.; Wang, L.; Tan, T.Z.; Zhao, Y.; Zhang, Y.G. TiO2/GO-coated functional separator to suppress polysulfide migration in lithium-sulfur batteries. Beilstein J. Nanotechnol. 2019, 10, 1726–1736.
38. Xu, G.Y.; Yan, Q.B.; Wang, S.T.; Kushima, A.; Bai, P.; Liu, K.; Zhang, X.G.; Tang, Z.L.; Li, J. A thin multifunctional coating on a separator improves the cyclability and safety of lithium sulfur batteries. Chem. Sci. 2017, 8, 6619–6625.
39. Bhargav, A.; He, J.; Gupta, A.; Manthiram, A. Lithium-Sulfur Batteries: Attaining the Critical Metrics. Joule 2020, 4, 285–291.
40. Cheng, P.; Guo, P.Q.; Liu, D.Q.; Wang, Y.R.; Sun, K.; Zhao, Y.G.; He, D.Y. Fe3O4/RGO modified separators to suppress the shuttle effect for advanced lithium-sulfur batteries. J. Alloys Compd. 2019, 784, 149–156.
41. Lv, X.; Lei, T.; Wang, B.; Chen, W.; Jiao, Y.; Hu, Y.; Yan, Y.; Huang, J.; Chu, J.; Yan, C.; et al. An Efficient Separator with Low Li-Ion Diffusion Energy Barrier Resolving Feeble Conductivity for Practical Lithium–Sulfur Batteries. Adv. Energy Mater. 2019, 9, 1091800.
42. Zhao, M.; Peng, H.J.; Zhang, Z.W.; Li, B.Q.; Chen, X.; Xie, J.; Chen, X.; Wei, J.Y.; Zhang, Q.; Huang, J.Q. Activating Inert Metallic Compounds for High-Rate Lithium-Sulfur Batteries through In Situ Etching of Extrinsic Metal. Angew. Chem. 2019, 58, 3779–3783.
43. Zhang, H.Y.; Dai, R.Q.; Zhu, S.; Zhou, L.Z.; Xu, Q.J.; Min, Y.L. Bimetallic nitride modified separator constructs internal electric field for high-performance lithium-sulfur battery. Chem. Eng. J. 2022, 429, 132454.
44. Hong, X.J.; Song, C.L.; Yang, Y.; Tan, H.C.; Li, G.H.; Cai, Y.P.; Wang, H.X. Cerium Based Metal-Organic Frameworks as an Efficient Separator Coating Catalyzing the Conversion of Polysulfides for High Performance Lithium-Sulfur Batteries. ACS Nano 2019, 13, 1923–1931.
45. Peng, L.; Yu, Z.J.; Zhang, M.K.; Zhen, S.Y.; Shen, J.H.; Chang, Y.; Wang, Y.; Deng, Y.F.; Li, A.J. A novel battery separator coated by a europium oxide/carbon nanocomposite enhances the performance of lithium sulfur batteries. Nanoscale 2021, 13, 16696–16704.
46. Wang, Z.; Feng, M.; Sun, H.; Li, G.R.; Fu, Q.; Li, H.B.; Liu, J.; Sun, L.Q.; Mauger, A.; Julien, A.M.; et al. Constructing metal-free and cost-effective multifunctional separator for high-performance lithium-sulfur batteries. Nano Energy 2019, 59, 390–398.